Science of the Total Environment 904 (2023) 166291

Contents lists available at ScienceDirect

Science of the Total Environment

journal homepage: www.elsevier.com/locate/scitotenv

Molecular characterization of dissolved organic matter in urban stormwater pond and municipal wastewater discharges transformed by the Florida red tide dinoflagellate *Karenia brevis*

Amanda Muni-Morgan [a,c], Mary G. Lusk [b,*], Cynthia Heil [c], Audrey H. Goeckner [d], Huan Chen [e], Amy M. McKenna [e,f], Patricia Scanlon Holland [c]

[a] *University of Florida, Gulf Coast Research and Education Center, School of Natural Resources and Environment, Wimauma, FL 33598, USA*
[b] *University of Florida, Gulf Coast Research and Education Center, Soil, Water, and Ecosystem Sciences Department, Wimauma, FL 33598, USA*
[c] *Mote Marine Laboratory, Sarasota, FL 34236, USA*
[d] *University of Florida, Soil, Water, and Ecosystem Sciences Department, 1692 McCarty Dr, Gainesville, FL 32603, USA*
[e] *National High Magnetic Field Laboratory, Florida State University Tallahassee, FL 32310, USA*
[f] *Department of Soil & Crop Sciences, Colorado State University, Fort Collins, CO 80523, USA*

HIGHLIGHTS

- DOM in urban stormwater pond and wastewater effluent is bioavailable to *K. brevis*.
- Younger ponds contain a larger pool of labile DOM to *K. brevis* vs. older ponds.
- The youngest stormwater pond contained more BDON than wastewater effluent.
- Depletions of DOM compounds correspond to amino sugars, lignin, and humic acids.

GRAPHICAL ABSTRACT

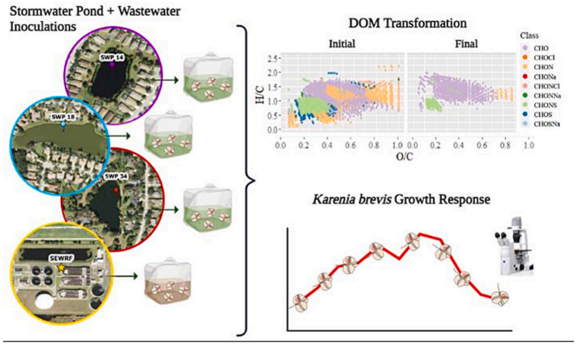

ARTICLE INFO

Editor: Shuzhen Zhang

Keywords:
Harmful algal blooms
Red tide
Stormwater ponds
Wastewater effluent
Dissolved organic nitrogen
FT-ICR MS

ABSTRACT

Karenia brevis blooms occur almost annually in southwest Florida, imposing significant ecological and human health impacts. Currently, 13 nutrient sources have been identified supporting blooms, including nearshore anthropogenic inputs such as stormwater and wastewater outflows. A 21-day bioassay was performed, where *K. brevis* cultures were inoculated with water sourced from three stormwater ponds along an age gradient (14, 18, and 34 yrs.) and one municipal wastewater effluent sample, with the aim of identifying biomolecular classes and transformations of dissolved organic matter (DOM) compounds used by *K. brevis*. All sample types supported *K. brevis* growth and showed compositional changes in their respective DOM pools. Fourier-transform ion cyclotron resonance mass spectrometry (FT-ICR MS) catalogued the molecular composition of DOM and identified specific compound classes that were biodegraded. Results showed that *K. brevis* utilized species across a wide range of compositions that correspond to amino sugars, humic, and lignin-like biomolecular classes. The

---

* Corresponding author.
E-mail address: mary.lusk@ufl.edu (M.G. Lusk).

https://doi.org/10.1016/j.scitotenv.2023.166291
Received 23 May 2023; Received in revised form 11 August 2023; Accepted 12 August 2023
Available online 14 August 2023

municipal wastewater and the youngest stormwater pond (SWP 14) effluent contained the largest pools of labile DOM compounds which were bioavailable to *K. brevis*, which indicates younger stormwater pond effluents may be as ecologically important as wastewater effluents to blooms. Conversely, generation of DOM compounds of greater complexity and a wide range of aromaticity was observed with the older (SWP 18 and SWP 34) stormwater pond treatments. These data confirm the potential for stormwater ponds and/or wastewater to contribute nutrients which can potentially support *K. brevis* blooms, revealing the need for improved nutrient retention strategies to protect coastal waters from the potential ill effects of urban effluent.

1. Introduction

The coast of southwest Florida is plagued by near annual blooms of *Karenia brevis*, the toxic dinoflagellate responsible for Florida red tide. *Karenia brevis* is a harmful algal bloom (HAB) species that produces a suite of neurotoxins called brevetoxins, which can cause massive fish kills and mortality to other marine biota (e.g., dolphins and manatees, sea turtles, and seabirds) (Larkin and Adams, 2013). Brevetoxins can become aerosolized via sea spray, at which point they are subject to inhalation, causing problems for individuals suffering from respiratory ailments such as chronic obstructive pulmonary disease (COPD) and asthma (Fleming et al., 2005). Blooms of *K. brevis* not only impact the health of humans and wildlife, but can result in significant economic impacts (Larkin and Adams, 2013), including loss of fisheries and tourism, drops in coastal property values, and mitigation costs associated with cleaning up fish kills.

Determining the role of specific land-based nutrient sources supporting nearshore blooms of *K. brevis* is complex due to the variety of inputs that can contribute variable amounts of nitrogen (N) and phosphorus (P) that can satisfy requirements of blooms of varying magnitudes (Heil et al., 2014). In nearshore coastal waters, allochthonous inputs from the atmosphere as well as nutrients from the surrounding watersheds via rivers have been identified as nutrient sources to blooms (Heil et al., 2014). For example, in coastal areas the combined flux of N and P from Tampa Bay, Charlotte Harbor, and the Caloosahatchee River can contribute 11–50 % N and 11–57 % P, capable of sustaining moderately sized blooms (3×10^5 cells L^{-1}) (Vargo et al., 2008). Results from a stable isotopic analysis ($\delta^{15}N$ and $\delta^{13}C$) of particulate organic matter (POM) associated with coastal *K. brevis* blooms showed a range of signatures corresponding to fertilizer, sewage and atmospheric DIN, suggesting blooms utilize a mixture of estuarine sources of nutrients (Havens, 2004).

Historically, there has been an emphasis on inorganic N species such as nitrate (NO_3^-), and ammonium (NH_4^+) supporting *K. brevis* bloom populations (Killberg-Thoreson et al., 2014a) despite the bulk of N in estuarine, coastal, and offshore waters being in the form of dissolved organic nitrogen (DON) (Vargo et al., 2008). Southwest Florida coastal waters are generally considered N limited due to low concentrations of dissolved inorganic N (DIN) (Vargo et al., 2008; Vargo et al., 1992; Fraser and Wilcox, 1981). Contrarily, concentrations of dissolved organic N (DON) in southwest FL regions prone to recurrent blooms of *K. brevis* can be orders of magnitude greater than DIN, with concentrations up to 56 μM in Tampa Bay and Charlotte Harbor (Vargo et al., 2004) and typically 8 to 14 μM in coastal waters where *K. brevis* blooms (Vargo et al., 2008). The degree to which DON and other dissolved organic compounds from land-based sources are utilizable by *K. brevis* is poorly constrained. Investigating the role of DON and other dissolved organic matter (DOM) compounds in supporting *K. brevis* growth is principal to understanding how blooms are so successful once entering coastal waters. *Karenia brevis* is a mixotrophic alga, which means it is capable of utilizing both inorganic and organic forms of nutrients in dissolved (Heil et al., 2014; Killberg-Thoreson et al., 2014a) and particulate (Glibert et al., 2009) forms. For example, bloom populations have been shown to take up DON in the form of urea and amino acids (Heil et al., 2014; Bronk et al., 2014) as well as DON compounds excreted by the co-occurring diazotroph *Trichodesmium* (Bronk et al., 2014; Sipler et al., 2013). The role of DOM, however, is less understood as DOM can contain not only N but other elements that may be labile to *K. brevis*. Adding to this enigma is the potential role that urban effluent sources such as stormwater runoff, wastewater, or effluent from stormwater conveyances such as stormwater ponds play in providing bioavailable DOM to *K. brevis*.

Urban watersheds can transport large quantities of N downstream via stormwater runoff which can convey N from fertilizer application, animal waste, vegetation, atmospheric deposition, and biological N fixation (Hobbie et al., 2017; Lusk et al., 2023; Lusk et al., 2020). In addition to N, engineered drainage networks can convey large fluxes of organic carbon and sulfur compounds (Kaushal and Belt, 2012) which can be used for algal metabolism. In the state of Florida, there are over 76,000 urban stormwater ponds, and many more in other urbanized areas of the world (Sinclair et al., 2020). They are designed to mitigate the flooding threats of increased imperviousness in urban landscapes and are commonly hydrologically connected to receiving waters, meaning that any pollutant loads in their outflows are carried to nearby streams, estuaries, and bays. In this way, stormwater ponds may be viewed as a junction between built and natural environments, either buffering downstream waters from stormwater pollution or conversely funneling stormwater pollution downstream if the ponds are not able to achieve desired pollution removal. However, while stormwater ponds are usually expected to perform some level of pollutant removal (Collins et al., 2010) to protect downstream receiving waters, a growing body of evidence indicates that stormwater ponds are poor removers of nutrients and may be net exporters of dissolved nutrients (Rosenzweig et al., 2011) including bioavailable DON (BDON) (Lusk and Toor, 2016a). This can happen when organic nutrients associated with pond sediments are mineralized and remobilized to the water column. For example, previous studies have shown that bacteria inoculated with stormwater runoff and pond outflow water contain 10–40 % BDON, respectively (Lusk and Toor, 2016a; Jani et al., 2020), and coastal detention ponds along an urban gradient can promote HABs, including blooms of *Gymnodinium* sp. (Lewitus et al., 2008).

In addition to outflows from urban stormwater ponds, treated wastewater effluent is another component of the urban water cycle that contains elevated nutrient levels that are often released into coastal waters. Florida leads the nation in beneficial reuse of treated wastewater effluent (also called reclaimed water), reusing approximately 908 million gallons day^{-1} in 2022, primarily for irrigation of agricultural and urban lands (FDEP, 2020). However, this is only 53 % of the state's current domestic wastewater flow (FDEP, 2020). The remaining unused wastewater effluent is disposed of via rapid infiltration basins, injection wells or released into surface waters (Young and York, 1996). The total N content within domestic wastewater effluent varies between 10 and 20 mg L^{-1} depending on the level of treatment (Chen et al., 2013), and the material therein is comprised of a heterogeneous mixture that includes DOM, pharmaceuticals, and anthropogenic materials (Wang et al., 2018). DOM levels can be considerably high in treated effluent, which can be problematic as materials such as fulvic acids can complex with chemical compounds such as chlorine forming disinfection byproducts (DBPs) (Janhom et al., 2009). DBPs produced via chlorination including trihalomethane and haloacetic acids are of particular concern because of their carcinogenic effects upon exposure (Rook, 1976). Additionally, wastewater discharges have been shown to stimulate the growth of algae via contributions of labile DON (Bronk et al., 2010). In terms of *K. brevis*, additions of wastewater have been shown to stimulate growth three-fold when compared to controls and equivalent individual additions of inorganic N and P alone (Doig and Martin, 1974).

Fourier transform ion cyclotron resonance mass spectrometry (FT-ICR MS) is the only mass spectral technique that can achieve ultrahigh resolving power across a wide molecular weight range, sufficient to enable identification of tens of thousands of ionized species (Kujawinski, 2002). The benefit of electrospray ionization coupled with FT-ICR MS is it is considered a “soft” ionization technique, which leaves polar macromolecules intact (Fievre et al., 1997). This analytical technique does not, however, provide information on isomeric structure unless paired with additional analyses such as nuclear magnetic resonance (Kujawinski, 2002), and subsequent molecular formulae may be representative of various isomers. FT-ICR MS has been utilized to compare changes in DOM composition before and after algal or bacterial bioassays. For example, the use of FT-ICR MS facilitated the discovery that cellular exudates derived from the N fixing cyanobacterium *Trichodesmium* are bioavailable to *K. brevis* and serve as an important nutrient source in offshore oligotrophic waters (Sipler, 2009). Further, FT-ICR MS was used to evaluate the composition of DOM from decaying fish that serve as a nutrient source for *K. brevis* blooms (Killberg-Thoreson et al., 2014b). In the case of this study, FT-ICR MS enables comparison of DOM compound utilization by *K. brevis* when inoculated with different urban effluent types, providing insight into bioavailable compounds and potential degradation products.

The purpose of this study was to characterize the DOM utilization from stormwater pond and wastewater effluent by a *K. brevis*-bacterial assemblage and apply FT-ICR MS to catalogue the molecular composition of DOM compounds consumed by *K. brevis.* The complex nature of DOM in urban stormwater ponds and municipal wastewater (biogeochemical source material, diagenetic state) necessitates high resolution analyses to identify the chemical composition of these effluent sources and measure the potential bioavailability to *K. brevis*. We hypothesize that nearshore Florida waters impacted by municipal wastewater discharges and outflows of urban stormwater ponds will contribute a pool of bioavailable DOM to *K. brevis* and that specific compound classes utilized in the DOM pool can be identified through FT-ICR MS analysis. We are aware of no other studies that have investigated the molecular structure of compounds in stormwater or wastewater DOM that are utilized by *K. brevis*.

2. Materials and methods

2.1. Site description

Water samples were collected from the outflows of three stormwater ponds and one wastewater treatment plant in November 2019 (Fig. S1) in the Bradenton, Florida metropolitan area. The stormwater ponds are all in urban residential communities, varying in age (14, 18, and 34 years, SWP 14, SWP 18, and SWP 34, respectively). These ponds are wet retention ponds designed to receive and hold stormwater runoff from adjacent impervious surfaces and are hydrologically connected via stormwater pipes to the Braden River, a tributary of the Manatee River and part of the Tampa Bay watershed. Outflows from the ponds are directed to the Braden River when pond water levels exceed a specified threshold (see pond morphological properties, Table S1).

The municipal wastewater effluent sample (MWW) was received from the Southeast Water Reclamation Facility (SEWRF) in Bradenton, FL. This facility is a conventional wastewater treatment plant (at the time of collection, 2019) with a treatment capacity of 11 million gallons day^{-1} and supplies the adjacent urban residential communities with reclaimed water. The final step in wastewater treatment at the SEWRF is a chlorine contact chamber that achieves water disinfection prior to reuse for irrigation. A storage pond collects and holds treated wastewater onsite prior to distribution to the nearby urban area for lawn and green space irrigation. When the volume of water treated at the facility exceeds the pond's storage capacity due to heavy rainfall, excess water is discharged to natural surface waters that drain to Sarasota Bay.

2.2. Wastewater and stormwater collection

The MWW sample (1 L) was provided by SEWRF and collected from a release valve onsite used for water quality monitoring. Triplicate stormwater pond samples were collected from the outfall areas of each pond by dipping 250 mL high-density polyethylene collection bottles ~5 cm below the pond surfaces. Sample bottles were stored on ice for transport back to the laboratory and analyzed within 48 h. for total dissolved organic carbon (DOC) and total dissolved nitrogen (TDN) with a Shimadzu TOC/Total N analyzer (Table 2).

2.3. Bioassay experiments

Karenia brevis cultures (Mote Manasota clone) were maintained in L1 medium (modified by the omission of Si) under a 12:12 light:dark cycle at 24 °C. For the bioassay experiment, a *K. brevis* culture was diluted to $\sim 1 \times 10^6$ cells L $^{-1}$ with filtered (Whatman® 0.2 μm Nuclepore filters) seawater collected from Mote's New Pass dock (salinity, 32 ppt). Triplicate samples (2 L) of dilute culture were placed into cleaned (10 % HCl rinse followed by three DIW rinses) 4 L cubitainers and inoculated with 75 mL of filtered (Whatman 0.2 μm Nuclepore filters) effluent, the optimal volume determined to maintain pH and salinity at ~8.2 and 31.5 ppt. All treatments were incubated at 24 °C under a 12:12 light: dark cycle in a Thermo Scientific™ Precision™ Plant Growth Chamber. Photosynthetically active radiation (PAR) within cubitainers ranged from 83 to 135 μmol m^{-2} s^{-1} and was measured using a WALZ US-SQS/L Spherical Micro Quantum Sensor. Cell concentrations were sampled every 24 h. and preserved (Lugol's Solution) for later microscopic enumeration using a Zeiss Axio Vert.A1. The bioassay was terminated after 508 h. when cell concentrations declined.

2.4. Molecular characterization by negative-ion ESI FT-ICR MS

Samples were prepared for FT-ICR MS based on modification of the Dittmar method reported previously (Lusk and Toor, 2016a; Dittmar et al., 2008). In brief, 20 mL samples were collected from each treatment at 0 and 264 h. timepoints (T_0 and T_{264}, respectively) with the latter corresponding to late stationary phase. This timepoint was chosen to minimize measurement of DOM compounds due to release upon cell lysis during the termination phase, enabling identification of degradation products produced by *K. brevis*. Samples were filtered (pre-combusted Whatman® 0.7 μm GF/F filters) then concentrated by passing through 1 g, 6 mL Agilent Bond Elut PPL (styrene-divinylbenzene) solid phase extraction cartridges and eluted with HPLC-grade methanol. The eluate was frozen (−20 °C) until ready for negative-ion ESI FT-ICR MS analysis at the National High Magnetic Field Laboratory (NHMFL) in Tallahassee, FL with a custom-built FT-ICR mass spectrometer equipped with a 9.4 T superconducting solenoid magnet (Kaiser et al., 2011a; Chen et al., 2014a; Kaiser et al., 2014a). SPE extracts were ran at 50 ppm carbon in methanol prior to analysis by negative ion electrospray ionization. Sample solution was infused via a microelectrospray source (Emmett et al., 1998) (50 μm i.d. fused silica emitter) at 500 nL/min by a syringe pump. Typical conditions for negative ion formation were: emitter voltage, −2.4-2.9 kV; tube lens, −250 V; and heated metal capillary current, 7 A.

Ions were initially accumulated in an external multipole ion guide (1–5 ms) and released *m/z*-dependently by decrease of an auxiliary radio frequency potential between the multipole rods and the end-cap electrode (Kaiser et al., 2014b). Ions were excited to *m/z*-dependent radius to maximize the dynamic range and number of observed mass spectral peaks (32–64 %) (Kaiser et al., 2013), and excitation and detection were performed on the same pair of electrodes (Chen et al., 2014b). The dynamically harmonized ICR cell in the 9.4 T FT-ICR is operated with 6 V trapping potential (Boldin and Nikolaev, 2011; Kaiser et al., 2011b). Time-domain transients of 7.2 s were acquired with the Predator data station, with 100 time-domain acquisitions averaged for all experiments (Blakney et al., 2011).

Mass spectra were internally calibrated with five high-abundance homologous series that span the sample molecular weight distribution based on the "walking" calibration method (Savory et al., 2011). Experimentally measured masses were converted from the International Union of Pure and Applied Chemistry (IUPAC) mass scale to the Kendrick mass scale (Kendrick, 1963) for rapid identification of homologous series for each heteroatom class (i.e., species with the same $C_cH_hN_nO_oS_s$ content, differing only be degree of alkylation) (Hughey et al., 2001). Assigned peaks were limited to the following elemental composition based on isotopic fine structure confirmation: $C_{0\text{–}100}$ $H_{0\text{–}150}$ $O_{0\text{–}40}$ $N_{0\text{–}4}$ $S_{0\text{–}3}$. For each elemental composition, $C_cH_hN_nO_oS_s$, the heteroatom class, type (double bond equivalents, DBE = number of rings plus double bonds to carbon, DBE $= C - h/2 + n/2 + 1$) (McLafferty and Turecek, 1993) and carbon number, c, were tabulated for subsequent generation of heteroatom class relative abundance distributions and graphical relative-abundance weighted images and van Krevelen diagrams. Peaks with signal magnitude >6 times the baseline root-mean-square (rms) noise at m/z 500 were exported to peak lists, and molecular formula assignments and data visualization were performed with PetroOrg © software (Corilo, 2014). Each mass spectrum was internally calibrated for absorption mode data processing, and mass spectral peaks with $>6\sigma$ were exported to a peak list. Molecular formula assignments with an error of >0.5 ppm were discarded, and chemical classes with combined relative abundance of ≥0.15 % of the total with a minimum of 3 peaks per homologous series remained. Chloride and sodium adducts were detected in all samples (Table S3) but were excluded from this analysis.

2.5. *Statistical analysis*

Data analysis of peaks was performed using PetroOrg© and 'RStudio' (version 4.2.2) software. The PetroOrg© software used for FT-ICR MS data processing is publicly available: https://nationalmaglab.org/user-facilities/icr/software/. All data sets shown herein are publicly available via the Open Science Framework at https://osf.io/n8mza/ (DOI 10.17605/OSF.IO/N8MZA). Peak assignment settings for all compounds in downstream analysis were set to a maximum double bond equivalency (DBE) of 50, an error of 1 ppm, a minimum of 3 peaks per homologous series, and removal of compound classes <0.1 % of the total with any duplicated molecular formulae. All formulas unique to T_0 (not present in T_{264}) were denoted "T_0" with all formulas unique to T_{264} (not present in T_0) denoted "T_{264}". Due to the reproducibility of FT-ICR MS peak magnitude (Sleighter et al., 2012) and peak detection (Soule et al., 2010) between replicate samples, one sample was chosen at random to be representative of each effluent treatment.

A modified aromaticity index (AI_{mod}) was calculated to estimate the aromaticity of each molecular formula measured at T_0 and T_{264} using the sum of the relative abundance for each compound class (i.e., CHO, CHON, CHOS, CHONS). The index was calculated using the following equation:

$$AI_{mod} = \frac{1 + C - 0.5O - S - 0.5(N + H)}{C - 0.5O - N - S} \tag{1}$$

where C, H, O, N, and S represent the total number of atoms (carbon, hydrogen, oxygen, nitrogen, and sulfur, respectively) within a given molecular formula. AI_{mod} values were categorized as aliphatic ($AI_{mod} <$ 0.5), aromatic ($0.66 \geq AI_{mod} \geq 0.5$), and condensed aromatic ($AI_{mod} \geq$ 0.67) using thresholds outlined by Koch and Dittmar (2006).

A non-metric multidimensional scaling (NMDS) approach was employed using Bray-Curtis dissimilarity indices to assess the similarity or dissimilarity of each sample treatment, comparing the diversity of compounds by molecular formula and respective total abundance (peaks) of DOM compounds at T_0 and T_{264}. The total number of peaks measured for a molecular formula was considered as abundances, and the absence of a compound in a sample was given an abundance value of zero. Compounds were removed from analysis if the total peak abundance across all treatments was less than five. Functions from the vegan package in Rstudio software were used to calculate dissimilarity indices, perform NMDS, and assess the stress and goodness of fit. Rstudio software was also used for statistical analysis of *K. brevis* cell counts.

2.6. *Nutrient analysis*

At T_0 and T_{264} 300 mL from each treatment was collected and filtered (pre-combusted Whatman® 0.7 μm GF/F filters), sub-sampled into low-density polyethylene (LDPE) centrifuge tubes (Corning®), and frozen (−20 °C) for later analysis of dissolved organic carbon (DOC), total dissolved nitrogen (TDN), and DIN (sum of NH_4^+ and nitrate + nitrite (NO_x^-)). DOC and TDN concentrations were measured via combustion catalytic oxidation using a Shimadzu TOC-L analyzer. Ammonium and nitrate + nitrite were analyzed using the salicylate method (Seal method G-102-93) and sulphanilamide method (Seal method G-109-94), respectively and were measured colorimetrically using a Seal AA3 continuous segmented flow analyzer. DON was calculated as the difference between TDN and DIN.

3. Results and discussion

3.1. *Bulk DOM characterization and transformation by Karenia brevis*

Negative-ion ESI FT-ICR MS analysis identified 3188 to 10,776 DOM compounds at T_0, and 1911 to 11,465 compounds at T_{264} (Table 1). There was a measured increase in average DOC concentrations within each treatment at T_{264} (Table 2), with observed qualitative changes in DOM biomolecular classes (Fig. 1). CHO and CHON compounds were the most abundant compound classes across all treatments, followed by sulfur (S) containing compounds. This is in line with previous work that characterized chemical classes in bulk DOM from wastewater effluent, urban stormwater runoff and urban streams (Lusk and Toor, 2016a; Lusk and Toor, 2016b; Zhang et al., 2021).

Assigned formulas were plotted using van Krevelen diagrams which assign estimates of biogeochemical classes by plotting the molar oxygen: carbon (O/C) ratio versus the molar ratio of hydrogen:carbon (H/C)

Table 1

Comparison of total peak number for each compound class and percent relative abundance across each bioassay sample treatment. T_0 and T_{264} are denoted next to Sample ID.

Sample ID	Compound class				
	CHO	CHON	CHOS	CHONS	Total Peaks
SWP 14 T0	4512 (42 %)	4568 (42 %)	1696 (16 %)	0	10,776
SWP 14 T264	1815 (34 %)	2814 (53 %)	688 (13 %)	0	5317
SWP 18 T0	2983 (39 %)	3440 (44 %)	1310 (17 %)	0	7733
SWP 18 T264	4472 (39 %)	4712 (41 %)	2281 (20 %)	0	11,465
SWP 34 T0	1780 (56 %)	656 (21 %)	752 (24 %)	0	3188
SWP 34 T264	3146 (57 %)	1258 (23 %)	1162 (21 %)	0	5566
MWW T0	2231 (35 %)	2319 (37 %	1191 (19 %	560 (9 %)	6301
MWW T264	1178 (62 %)	431 (23 %)	282 (15 %)	20 (1 %)	1911

Table 2
Mean concentrations of total dissolved nitrogen (TDN), dissolved inorganic nitrogen (DIN), dissolved organic nitrogen (DON), and dissolved organic carbon (DOC) in municipal wastewater (MWW) and stormwater pond (SWP) treatments. Means are averaged from each triplicate.

Sample ID	Sampling hour	TDN (mg L^{-1})	DIN (mg L^{-1})	DON (mg L^{-1})	DOC (mg L^{-1})
MWW	0	4.06	1.67	2.4	15.13
MWW	264	2.97	1.07	1.9	16.17
SWP 14	0	3.4	1.32	2.08	15.57
SWP 14	264	2.7	1.26	1.45	16.4
SWP 18	0	3.4	1.35	2.05	15.37
SWP 18	264	3.47	1.5	1.96	17.0
SWP 34	0	3.2	1.38	1.82	15.03
SWP 34	264	3.13	1.29	1.86	16.1

(Fig. 1) (Kim et al., 2003). In terms of relative peak abundance, CHO compounds accounted for 35–56 % of all compounds at T_0 and 34–62 % of all compounds at T_{264}. DOM in the form of carbohydrates are an important component of marine carbon cycles, as they make up most of the DOM that is released by phytoplankton in the form of exopolymers (Biddanda and Benner, 1997). Production of DOC was observed across all treatments at T_{264} (Table 2), suggesting that introductions of urban effluent may induce the release of labile photosynthate by phytoplankton which has important implications for bacterial mineralization of DOM and the microbial loop (Azam et al., 1983). The CHO compounds in this bioassay correspond to various regions on the van Krevelen diagram across all treatments (Fig. 1) including lignin, unsaturated hydrocarbons, proteins, and carboxyl-rich alicyclic molecules (CRAM), highlighting the diversity of this DOM class. CRAM-like molecules are a group of recalcitrant organic compounds comprised of carboxylated and fused alicyclic rings that have structural similarities to

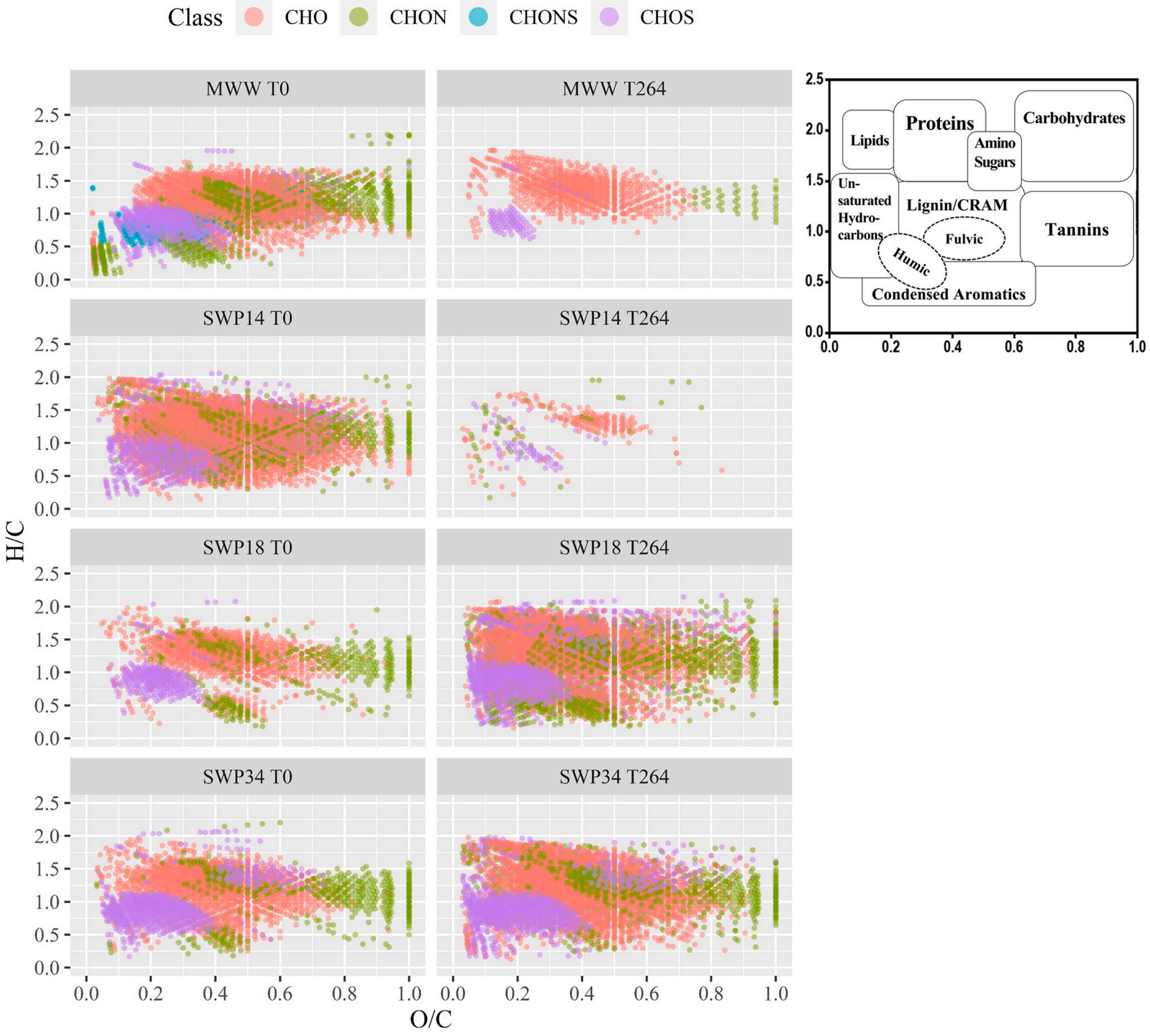

Fig. 1. van Krevelen diagrams displaying measured peaks for each effluent type comparing compounds unique to T_0 ('removed') vs. compounds unique to T_{264} ('produced'). The H/C vs. O/C values can be correlated to a biomolecular class as placed to the upper-right for reference modified from Sleighter and Hatcher (2011), with the addition of carboxyl-rich alicyclic molecules (CRAM) (Hertkorn et al., 2006) as well as humic and fulvic acids (Kovács et al., 2010).

terrestrial humic compounds (Nebbioso et al., 2014). The AI_{mod} values (Fig. 3) indicate that CHO compounds consumed and produced across all treatments are mostly aliphatic. A reduction of total CHO peaks was observed in the MWW and SWP 14 treatments at T_{264} (Fig. 1). An opposite pattern was observed with additions of effluent from the two older ponds with variable changes in average molecular weight (Fig. 2), suggesting compounds from MWW and SWP 14 are more labile across a range of masses. The relative increases in CRAM-like CHO peaks for SWP 18 and SWP 34 treatments suggest the production of biomolecules that are more refractory which is supported by the higher percentage of the AI_{mod} defined classes of aromatic and condensed compounds at T_{264}.

The presence and transformations of CHOS compounds was observed in all treatments (Fig. 1). CHOS compounds in the MWW and SWP 14 treatments decreased >50 % from T_0 to T_{264} (Table 1), suggesting that a majority of these compounds were consumed or degraded during the bioassay. Conversely, increases of CHOS compounds at T_{264} in SWP 18 and SWP 34 were observed (Table 1; Fig. 1). This could be due to the production of the organosulfur metabolite DMSP (Dimethylsulfoniopropionate, molecular formula $C_5H_{10}O_2S$) by *K. brevis* (Van Dolah et al., 2009) which can serve as an antioxidant and become induced upon oxidative stress (Sunda et al., 2002). Xenobiotics applied in urban environs that can induce oxidative stress include the aquatic herbicides Sethoxydim ($C_{17}H_{29}NO_3S$) and Topramezone ($C_{16}H_{17}N_3O_5S$) which are approved for use in Florida and are commonly used for weed control (Langeland, 2014). However, the application of these specific chemicals in areas surrounding SWP 18 and SWP 34 has not been confirmed. A greater percentage of aromatic and condensed aromatic compounds were consumed and produced in SWP 18 and SWP 34 (Fig. 3), indicating older stormwater ponds can be both a source and sink of aromatic DOM. Other sources of S include anthropogenic emissions which contribute more S than natural sources (i.e., weathering) by a factor of 3 or 4 (Giordano et al., 2005). Subsidies of S from emissions, along with contributions from wastewater including surfactants and their degradation products (Gonsior et al., 2011), can substantially increase the S content of freshwater systems (Holmer and Storkholm, 2001). While bulk measurements of S were not performed in this study, these results show that wastewater and stormwater ponds may serve as an important source of S to coastal waters by influencing the ecophysiology of *K. brevis*.

3.2. Insights into dissolved organic N transformations

Numerous studies have investigated the bioavailability and environmental implications of DON in municipal wastewater effluents (e.g., Wang et al., 2023; Hu et al., 2022; Yan et al., 2022 and citations therein), but such studies are still limited for stormwater or stormwater pond effluents (Lusk and Toor, 2016a; Jani et al., 2020). Southwest Florida coastal waters are considered N-limited, and the N-bearing organic compounds in effluent treatments within this study may be expected to have varying degrees of bioavailability, so it is important to further characterize this DON component. Changes in the molecular weight distribution of N-bearing compounds consumed and produced by *K. brevis* (Fig. 2) are also described, as molecular weight distribution can be an indicator of expected lability for DON compounds (Yang et al., 2021). For example, high molecular weight compounds such as humic acids have been shown to be taken up by *K. brevis* (Killberg-Thoreson et al., 2014a). Further, phytoplankton can also take up small molecules such as dissolved free amino acids (Seitzinger et al., 2002).

CHON compounds accounted for 21–44 % of all compounds in the samples at T_0 and 23–53 % of all compounds at T_{264}. Nitrogen in the organic form has been shown to be a major pool of total N in stormwater and stormwater ponds (Lusk et al., 2020; Jani et al., 2020), which is reflected in the SWP samples which are rich in N-bearing organic compounds (Table 1). The N in the SWP samples likely originates in part from catchment vegetation and soils, fertilizers, and microbial byproducts of in-pond biological transformations of N (Osburn et al., 2016; Williams et al., 2013). An increase in relative abundance of CHON compounds was observed in SWP 18 and SWP 34 treatments at T_{264}. These compounds shifted to various regions of the van Krevelen diagram (i.e., lignin/CRAM, carbohydrates, condensed aromatics) indicating an

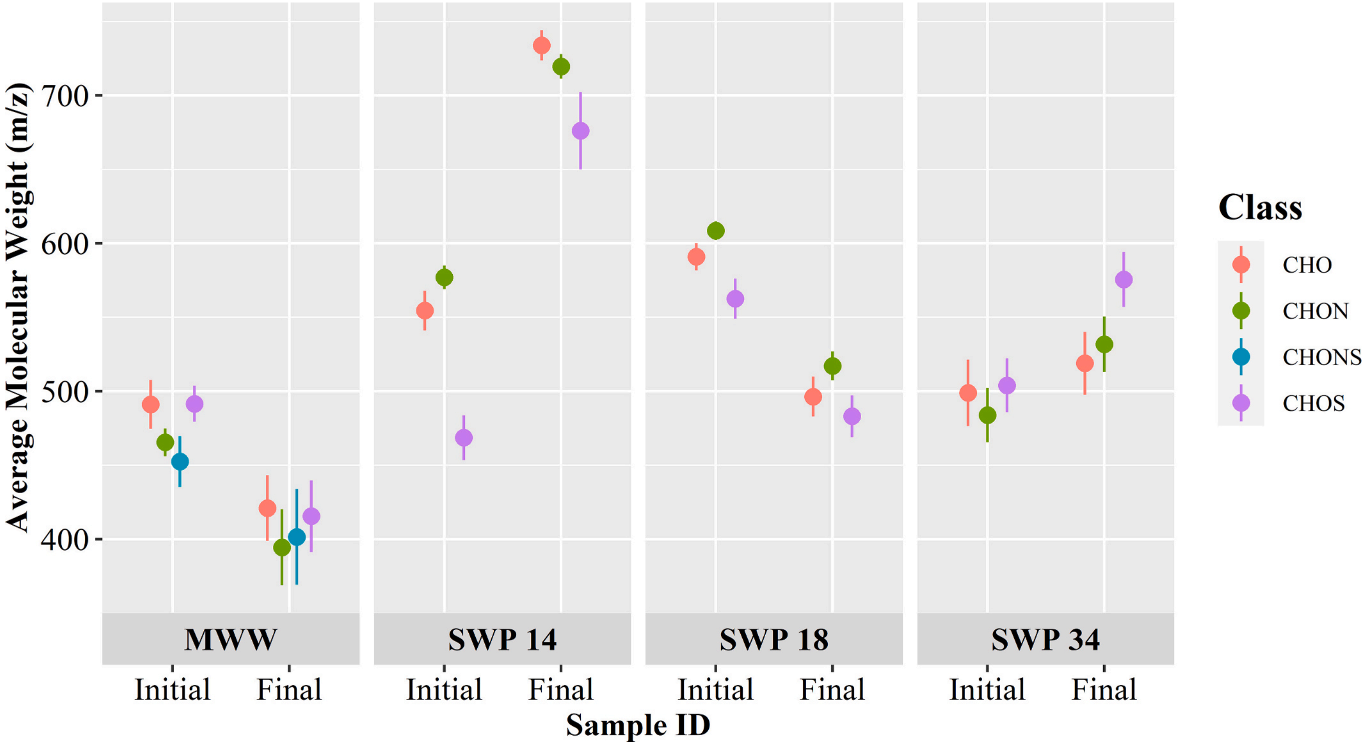

Fig. 2. Average molecular weight (*m/z*) distribution of DOM compounds unique to T_0 ('Initial') vs. compounds unique to T_{264} ('Final') among each effluent treatment. Colors represent respective DOM elemental classes. Vertical bars represent standard error of the mean.

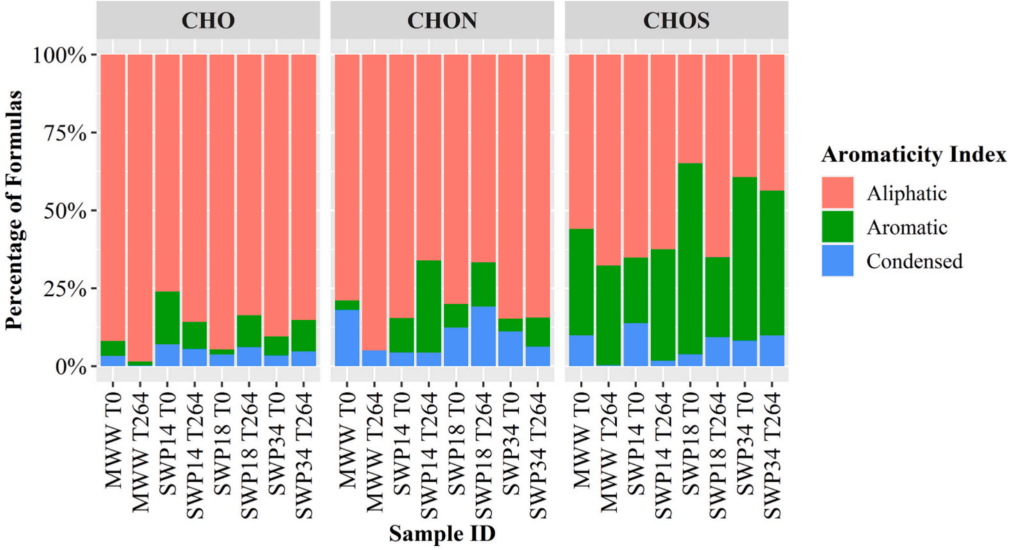

Fig. 3. Modified aromaticity index (AI_{mod}) of all molecular formulae measured at T_0 and T_{264}. The percentage of formulas is representative of the sum of the relative abundances for each compound class. AI_{mod} values were categorized as aliphatic ($AI_{mod} < 0.5$), aromatic ($0.66 \geq AI_{mod} \geq 0.5$), and condensed aromatic ($AI_{mod} \geq 0.67$) using thresholds outlined by Koch and Dittmar (2006). CHONS compounds were excluded from the figure as they were only detected in the MWW sample.

increase in compound complexity and was verified by resultant AI_{mod} values for T_{264} (Fig. 3). Conversely, a relative decrease in CHON compounds was observed in the MWW and SWP 14 treatments corresponding to lignin/CRAM, humic and fulvic biomolecular classes, indicating a higher degree of bioavailability in CHON compounds from these effluent sources. >75 % of compounds consumed at T_0 for the MWW and SWP 14 treatments were comprised of aliphatic compounds. Specific DON compounds common to wastewater effluent include free and combined amino acids (Pehlivanoglu-Mantas and Sedlak, 2008) and other low molecular weight compounds including peptidoglycans from bacterial cell walls (Dignac et al., 2000). This is evident in the MWW treatment, which exhibited the lowest average molecular weight among all treatments (Fig. 2), and depletions in amino sugar and carbohydrate compounds.

CHONS compounds were detected by FT-ICR MS in the MWW effluent treatment only, with notable depletions observed in T_{264} which correspond to humic-like DOM (Table 1, Fig. 1). While not pictured in Fig. 3., AI_{mod} values for these compounds indicate that they were equally aliphatic and aromatic in structure. CHONS compounds in the MWW sample likely originate from dissolved organosulfur compounds such as detergents, surfactants, and pharmaceuticals which are ubiquitous in wastewater effluent (Liu et al., 2023). During oxic stages of the wastewater treatment process, labile, low-molecular weight CHONS compounds can be formed by copiotrophic bacteria, such that wastewater effluents are enriched in CHONS compounds relative to their influents (Liu et al., 2023). The CHONS compounds from wastewater may provide a potential source of amino acids, in addition to vitamins and cofactors for *K. brevis* growth, suggesting that wastewater treatment processes that can remove CHONS compounds would be advantageous in terms of bloom mitigation. Tertiary treatment processes that use coagulants with a higher degree of polymerization than those traditionally used in wastewater treatment have been shown to be effective in improving CHONS removal from effluents (Geng et al., 2018), and future work should be done to investigate the role that these coagulants may play in reducing pools of bioavailable DOM in wastewater effluent.

SWP 18 and SWP 34 exhibited overall increases in the number of N-containing compounds at T_{264} corresponding to the CHON biomolecular class during the course of the bioassay (Table 1), with a molecular weight of approximately 500 *m/z* (Fig. 2). The compounds that were produced by *K. brevis* when exposed to effluent from these ponds exhibit a more complex, and likely more recalcitrant pool of compounds such as lignin and CRAM molecules (Yang et al., 2021) (Fig. 1). An increase of newly-formed compounds within the lignin/CRAM biomolecular classes at T_{264} in SWP 18 and SWP 34 may also indicate partial mineralization of semi-labile DON, resulting in an increase of degradation products with greater recalcitrance, or the formation of DON compounds via de novo synthesis. However, it is important to note that the *K. brevis* cultures in our study were non-axenic, and the probability of bacterial remineralization of DON cannot be discounted, as the difficulty of maintaining axenic *K. brevis* cultures suggests that bacteria play a critical role in *K. brevis* nutrition. Increases in CHON at T_{264} could also be due to cellular lysis (Fig. 1), or exudation of dissolved amino acids by *K. brevis* and/or co-occurring bacteria.

To estimate the bioavailability of N-containing compounds within each effluent treatment, BDON was calculated using the difference of the mean initial and final DON concentrations (Table 2), and percent BDON was calculated by dividing BDON by the initial mean DON x 100. SWP 14 contained the largest pool of BDON (30 %), followed by the MWW treatment (21 %), SWP 18 (4 %) and SWP 34 (−2 %), respectively. These trends are evident in the van Krevelen diagrams (Fig. 1), where many compounds present at T_0 for MWW and SWP 14 are absent at T_{264}. The higher percentage of BDON in the MWW and SWP 14 treatments shows that these effluents contained a larger pool of DON compounds known to be bioavailable, corresponding to biomolecular groups such as carbohydrates and amino sugars (Sleighter and Hatcher, 2011) (Fig. 1). This BDON could include low molecular weight compounds such as urea and some amino acids which can be taken up by phytoplankton cells via active transport by use of a membrane sodium ion pump, by facilitated diffusion if extracellular concentrations are high (Capone et al., 2008), or by cell surface enzymes and oxidases (Palenik and Morel, 1990). Depletions in compounds corresponding to humic and fulvic acids were also observed, which agrees with previous studies measuring direct uptake of humic-N by cultures and natural bloom populations of *K. brevis* (Killberg-Thoreson et al., 2014a). Unsaturated hydrocarbon-like compounds, including aliphatic compounds were also depleted, which have been shown to be bioavailable to bacteria and phytoplankton (Yang et al., 2021; Yao et al., 2020).

It is noteworthy that the SWP 14 sample had the highest amount of BDON, more-so than the MWW sample, showing that stormwater ponds may be important sources of biologically reactive N to downstream waters, and can be comparable to wastewater effluents. It is also noteworthy that the youngest pond in our study contained a larger pool of

BDON than did the two older ponds, which could be due to previous microbial processing of DON. For example, SWP 34 had a history of cyanobacterial blooms (species unidentified) that proliferated prior to and during the sampling event. In a concomitant study on carbon cycling in the same ponds, it was shown that the SWP 14 (the youngest pond in the study) had a high rate of organic C mineralization that simultaneously increased C emissions from the pond while reducing organic C burial (Goeckner et al., 2022). It was further shown that as pond age increased, rates of organic C mineralization decreased (Goeckner et al., 2022), suggesting that older ponds have less organic C turnover than younger ponds, while results from this study add that they may also have less organic N turnover. Other studies on SWP N cycling also support successive biogeochemical shifts such that SWPs can either add more N to their pool via N_2 fixation (Gold et al., 2017) or remove inputs of N via denitrification (Hohman et al., 2021) with increasing pond age.

Even if N is delivered to stormwater ponds in an inorganic form, in-pond mineralization processes or microbial exudates may transform the overall N signature of stormwater ponds into a predominately organic form (Rosenzweig et al., 2011; Williams et al., 2013). In this way, stormwater pond effluents, which are hydrologically connected to downstream waters, may transport a large pool of DON ranging in bioavailability. For this study, the stormwater ponds had as much N-rich DOM compounds as did the wastewater effluent, highlighting one way that these ponds provide anthropogenic N subsidies to the downstream waters to which they are connected. While wastewater effluent discharges to receiving waters are rightly of concern from an N management perspective, these results show that stormwater ponds likely play an important role as well in N budgets within the urban water cycle.

3.3. *DOM compositional shifts revealed by NMDS*

NMDS ordination revealed compositional shifts of the DOM in all treatments comparing T_0 to T_{264} (Fig. 3). The resulting ordination exhibited goodness of fit with a stress value of 0.05, a linear R^2 of 0.967, and a non-metric R^2 fit of 0.995. NMDS analysis was performed using the total number of peaks for each measured molecular formula across all treatments, comparing compounds unique to T_0 ("consumed") and unique to T_{264} ("produced"). Counts for 403 unique DOM molecular formulae were considered for each treatment. The count matrix of the parameters total peak abundance and molecular formula for each treatment were used to calculate the dissimilarity distance between each sample, determining their coordinates on the ordination plot. Points that are clustered closely are more similar than points that are further apart. Further, the ordination of each molecular formula is plotted and is colored based on its' corresponding compound class, enabling visual inference of the DOM changes occurring between T_0 and T_{264}.

Results from the NMDS indicate that the molecular composition of compounds within the MWW are distinct from the stormwater ponds (Fig. 4). The MWW treatment also exhibited the largest distance between T_0 and T_{264}, indicating the greatest change in molecular composition. SWP 14 and SWP 18 treatments had the closest proximity, indicating a similar relative abundance of compounds with common molecular formulae. However, the composition of compounds shifted in opposite directions at T_{264}. This pattern could be attributed to the increase in compounds across all classes in the SWP 18 treatment measured at T_{264} (Table 1). Conversely, SWP 34 was the most dissimilar treatment at T_0 between all stormwater ponds. The direction of SWP 34 at T_{264} shifted towards the cluster of compounds produced at T_{264} within the SWP 18 treatment. This directional pattern suggests transformation and subsequent production of DOM compounds of similar molecular composition which mirrors the van Krevelen analysis (Fig. 1).

4. *Karenia brevis* growth response

Karenia brevis cells within all treatments responded to additions after 48 h. except for SWP 34, which exhibited no lag period in response (Fig. 5). Growth of cells was consistent between all samples until ~ T_{312}, where cell concentrations steadily declined until T_{508} when the experiment was terminated. A linear model was constructed to measure the potential significance of maximum cell concentrations between treatments, with log-transformed maximum cell abundance as the response variable and sample treatment as the predictor variable. Maximum cell concentrations in all treatments exceeded 2.0×10^6 cells L^{-1} (Table S2) and were not significantly different from each other ($p = 0.822$). Differences among specific growth rates, μ (day $^{-1}$) (Table S2) were tested using the emmeans package (emmeans: Estimated Marginal Means, aka

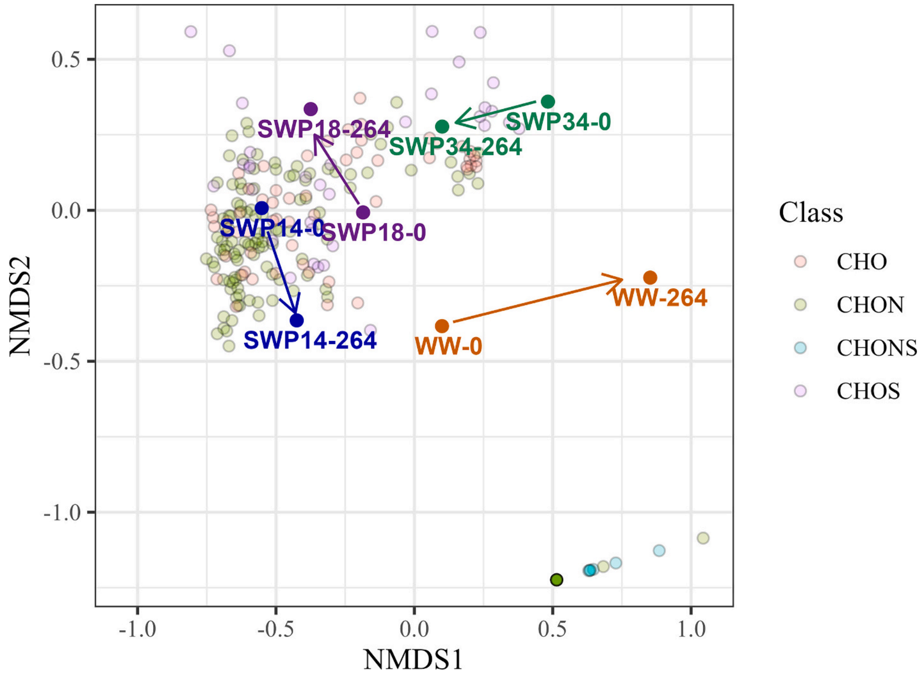

Fig. 4. NMDS ordination of samples before and after incubation (large, labelled circles). Arrows were added to highlight the directional shift in organic matter composition. Individual molecular formulae are plotted based on their variable scores (small translucent circles) and colored by their corresponding compound class.

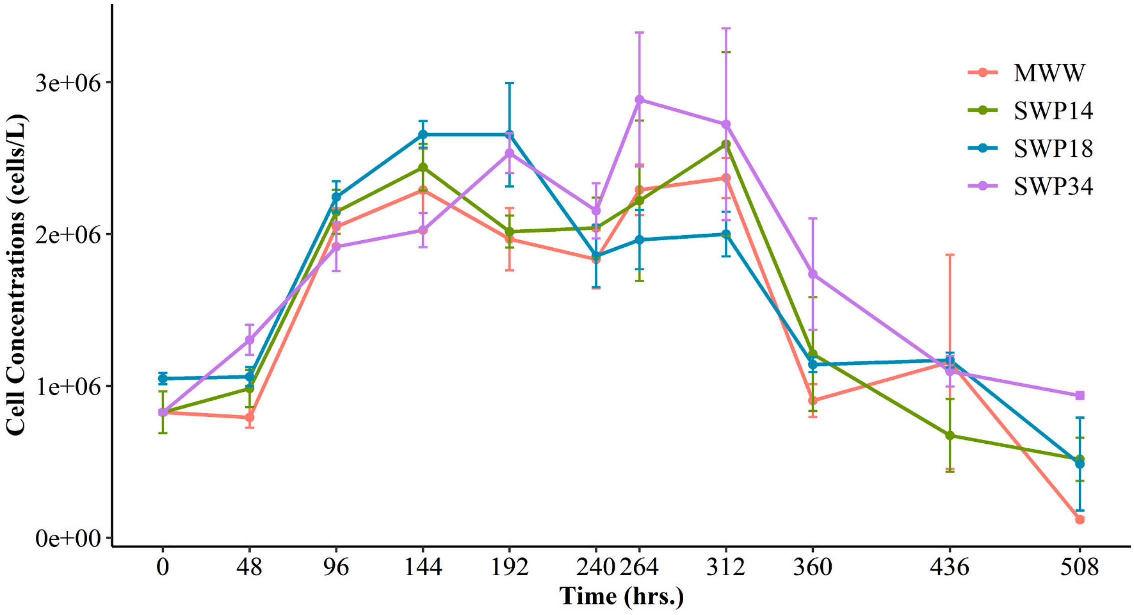

Fig. 5. Effects of municipal wastewater and stormwater effluent on *Karenia brevis* growth response. Each data point is the average of three replicates (±S.E.).

Least-Squares Means_. R package version 1.8.5, <https://CRAN.R-project.org/package=emmeans>.) which was used to calculate sample means and construct linear contrasts using a Tukey adjustment for multiple comparisons. Specific growth rates for MWW (mean 0.48 μ (day $^{-1}$)) were significant ($p < 0.013$) when compared to SWP 18 and SWP 34, but not significant between effluents MWW and SWP 14 ($p = 0.713$) or between treatments SWP 18 and SWP 34 ($p = 0.999$). These patterns in growth rates between effluent types correspond with the observed bioavailability of DOM compounds in each treatment, where MWW and SWP 14 contained the highest pools of BDON (21 and 30 %, respectively), and SWP 18 and SWP 34 contained the smallest pools of BDON (4 and − 2 %, respectively). Additionally, a 36 % reduction of DIN was observed for the MWW treatment at T_{264} which could have facilitated increased growth rates, while DIN was relatively unchanged for all pond treatments (Table 2). It is important to note that despite higher BDON in the MWW and SWP 14 treatments, SWP 18 and SWP 34 still resulted in the highest maximum cell concentrations (2.66×10^6 and 2.89×10^6 cells L^{-1}, respectively) observed at 144 and 264 h, respectively. As stated, there was no lag time observed for the SWP 34 treatment, and it had the highest maximum cell concentration. These results suggest that the DOM in each effluent treatment was utilized for *K. brevis* growth despite a varying range of bioavailability.

5. Conclusions

This work provides evidence of wastewater and urban stormwater pond DOM utilization and transformation by a *K. brevis*-bacteria consortia confirmed through bioassay and FT-ICR MS analysis. Florida's stormwater ponds and municipal wastewater effluent are relevant but overlooked sources of DOM reaching coastal waters. Consequently, environmental management and water quality monitoring efforts must expand to include analysis of DOM, including DON, which has not been traditionally recognized as part of the reactive N pool, and implement strategies of BDON fraction removal in wastewater and stormwater treatment technologies. Additionally, our study highlights that stormwater ponds may export as much BDON as wastewater effluents. Future research should focus on potential seasonal shifts and spatial trends in the DOM makeup of stormwater ponds, especially ponds hydrologically connected to downstream ecosystems.

This work underscores the importance of enhancing the DOM removal efficiencies of stormwater ponds and expanding the scope of flood mitigation to pollutant mitigation, as well as adopting advanced wastewater treatment technologies. CHONS compounds in MWW were highly bioavailable, suggesting that additions to tertiary treatment processes such as new coagulants to remove organosulfur compounds could be beneficial for water quality protection. Reduction and production of CHONS as well as CHOS compounds reveals that *K. brevis* plays an important role in the biogeochemical cycling of S from urban effluent, necessitating future research on the consequences of urban S subsidies to blooms. There was a net production of DOC by *K. brevis* across all treatments suggesting that introductions of DOM via urban effluent stimulate autochthonous production of DOM, which can provide an important carbon source for bacteria, fueling the microbial loop. Future research investigating the biogeochemical cycling of urban DOM, including the production and consumption by *K. brevis* and bacteria in coastal watersheds, is critical in understanding the fate of carbon and nutrients in bloom-impacted waters, which can ultimately aid in bloom prediction. Results from this study show that preventing wastewater and stormwater discharges to coastal waters can potentially play a role in mitigating *K. brevis* proliferation once a bloom reaches nearshore waters.

Funding sources

This research was made possible in part by a University of Florida Early Career Seed Grant to M. G. L., as well as support from the University of Florida Center for Land Use Efficiency; and funding for A. M-M. from the GCREC Scholarship Endowment from the University of Florida. Additional support was provided by NOAA Ecohab grant NA19NOS4780183, with additional salary support for C. A. H. from the Economos and Barancik Foundations. FT-ICR MS analysis was performed at the National High Magnetic Field Laboratory ICR User Facility, which is supported by the National Science Foundation Division of Chemistry and Division of Materials Research through (DMR-1644779) and the State of Florida. This is ECOHAB Publication #1076.

CRediT authorship contribution statement

Amanda Muni-Morgan: Data curation, Formal analysis, Investigation, Methodology, Visualization, Writing – original draft. **Mary G. Lusk:** Conceptualization, Funding acquisition, Investigation, Methodology, Project administration, Resources, Supervision, Writing – review & editing. **Cynthia Heil:** Conceptualization, Funding acquisition, Investigation, Methodology, Project administration, Resources, Writing – review & editing. **Audrey H. Goeckner:** Visualization, Formal analysis. **Huan Chen:** Methodology, Resources, Validation, Visualization, Writing – review & editing. **Amy M. McKenna:** Methodology, Resources, Validation, Visualization, Writing – review & editing. **Patricia Scanlon Holland:** Methodology, Resources, Writing – review & editing.

Declaration of competing interest

The authors declare the following financial interests/personal relationships which may be considered as potential competing interests: Mary Lusk reports financial support was provided by National High Magnetic Field Laboratory. Cynthia Heil reports financial support was provided by NOAA National Centers for Coastal Ocean Science Ecology and Oceanography of Harmful Algal Blooms Research Program.

Data availability

Data will be made available on request.

Acknowledgements

We express gratitude to Kylie Chapman for assistance in collecting the stormwater samples, as well as Stephen Suau who provided the reclaimed water sample.

Appendix A. Supplementary data

Supplementary data to this article can be found online at https://doi.org/10.1016/j.scitotenv.2023.166291.

References

Azam, F., et al., 1983. The ecological role of water-column microbes in the sea. Marine ecology progress series. Oldendorf 10 (3), 257–263.

Biddanda, B., Benner, R., 1997. Carbon, nitrogen, and carbohydrate fluxes during the production of particulate and dissolved organic matter by marine phytoplankton. Limnol. Oceanogr. 42 (3), 506–518.

Blakney, G.T., Hendrickson, C.L., Marshall, A.G., 2011. Predator data station: a fast data acquisition system for advanced FT-ICR MS experiments. Int. J. Mass Spectrom. 306 (2–3), 246–252.

Boldin, I.A., Nikolaev, E.N., 2011. Fourier transform ion cyclotron resonance cell with dynamic harmonization of the electric field in the whole volume by shaping of the excitation and detection electrode assembly. Rapid Commun. Mass Spectrom. 25 (1), 122–126.

Bronk, D.A., et al., 2010. Effluent organic nitrogen (EON): bioavailability and photochemical and salinity-mediated release. Environ. Sci. Technol. 44 (15), 5830–5835.

Bronk, D., et al., 2014. Nitrogen uptake and regeneration (ammonium regeneration, nitrification and photoproduction) in waters of the West Florida Shelf prone to blooms of *Karenia brevis*. Harmful Algae 38, 50–62.

Capone, D.G., et al., 2008. Nitrogen in the Marine Environment. Elsevier.

Chen, W., et al., 2013. Reclaimed water: a safe irrigation water source? Environ. Dev. 8, 74–83.

Chen, T., et al., 2014a. Note: optimized circuit for excitation and detection with one pair of electrodes for improved Fourier transform ion cyclotron resonance mass spectrometry. Rev. Sci. Instrum. 85 (6), 066107.

Chen, T., et al., 2014b. Note: optimized circuit for excitation and detection with one pair of electrodes for improved Fourier transform ion cyclotron resonance mass spectrometry. Rev. Sci. Instrum. 85 (6), 0666107/1–066107/3.

Collins, K., et al., 2010. Opportunities and challenges for managing nitrogen in urban stormwater: a review and synthesis. Ecol. Eng. 36 (11), 1507–1519.

Corilo, Y.E., 2014. PetroOrg Software, Omics, Editor. Florida State University, Omics LLC, Tallahassee, Fl.

Dignac, M.-F., et al., 2000. Determination of structure and origin of refractory organic matter in bio-epurated wastewater via spectroscopic methods. Comparison of conventional and ozonation treatments. Environ. Sci. Technol. 34 (16), 3389–3394.

Dittmar, T., et al., 2008. A simple and efficient method for the solid-phase extraction of dissolved organic matter (SPE-DOM) from seawater. Limnol. Oceanogr. Methods 6 (6), 230–235.

Doig, M., Martin, D., 1974. The response of *Gymnodinium breve* to municipal waste materials. Mar. Biol. 24 (3), 223–228.

Emmett, M.R., et al., 1998. Application of micro-electrospray liquid chromatography techniques to FT-ICR MS to enable high-sensitivity biological analysis. J. Am. Soc. Mass Spectrom. 9 (4), 333–340.

FDEP, 2020. 2020 Reuse Inventory (31 January 2022); Available from: https://floridadep.gov/sites/default/files/2020Reuse_Inventory_Report_Approved_2.pdf.

Fievre, A., et al., 1997. High-resolution Fourier transform ion cyclotron resonance mass spectrometry of humic and fulvic acids by laser desorption/ionization and electrospray ionization. Energy Fuel 11 (3), 554–560.

Fleming, L.E., et al., 2005. Initial evaluation of the effects of aerosolized Florida red tide toxins (brevetoxins) in persons with asthma. Environ. Health Perspect. 113 (5), 650–657.

Fraser, T.H., Wilcox, W.H., 1981. Enrichment of a subtropical estuary with nitrogen, phosphorus and silica. In: Estuaries and Nutrients. Springer, pp. 481–498.

Geng, C.-X., et al., 2018. Molecular characterization of organics removed by a covalently bound inorganic–organic hybrid coagulant for advanced treatment of municipal sewage. Environ. Sci. Technol. 52 (21), 12642–12648.

Giordano, M., Norici, A., Hell, R., 2005. Sulfur and phytoplankton: acquisition, metabolism and impact on the environment. New Phytol. 166 (2), 371–382.

Glibert, P.M., et al., 2009. Grazing by *Karenia brevis* on *Synechococcus* enhances its growth rate and may help to sustain blooms. Aquat. Microb. Ecol. 55 (1), 17–30.

Goeckner, A.H., et al., 2022. Florida's urban stormwater ponds are net sources of carbon to the atmosphere despite increased carbon burial over time. Commun. Earth Environ. 3 (1), 53.

Gold, A., Thompson, S., Piehler, M., 2017. Water quality before and after watershed-scale implementation of stormwater wet ponds in the coastal plain. Ecol. Eng. 105, 240–251.

Gonsior, M., et al., 2011. Molecular characterization of effluent organic matter identified by ultrahigh resolution mass spectrometry. Water Res. 45 (9), 2943–2953.

Havens, J.A., 2004. A Stable Isotopic Examination of Particulate Organic Matter during *Karenia brevis* Blooms on the Central West Florida Shelf: Hints at Nitrogen Sources in Oligotrophic Waters.

Heil, C.A., et al., 2014. Blooms of *Karenia brevis* (Davis) G. Hansen & Ø. Moestrup on the West Florida Shelf: nutrient sources and potential management strategies based on a multi-year regional study. Harmful Algae 38, 127–140.

Hertkorn, N., et al., 2006. Characterization of a major refractory component of marine dissolved organic matter. Geochim. Cosmochim. Acta 70 (12), 2990–3010.

Hobbie, S.E., et al., 2017. Contrasting nitrogen and phosphorus budgets in urban watersheds and implications for managing urban water pollution. Proc. Natl. Acad. Sci. 114 (16), 4177–4182.

Hohman, S.P., et al., 2021. Internal nitrogen dynamics in stormwater pond sediments are influenced by pond age and inorganic nitrogen availability. Biogeochemistry 156 (2), 255–278.

Holmer, M., Storkholm, P., 2001. Sulphate reduction and sulphur cycling in lake sediments: a review. Freshw. Biol. 46 (4), 431–451.

Hu, Q., et al., 2022. Using multiple isotopes to identify sources and transport of nitrate in urban residential stormwater runoff. Environ. Monit. Assess. 194 (3), 1–27.

Hughey, C.A., et al., 2001. Kendrick mass defect spectroscopy: a compact visual analysis for ultrahigh-resolution broadband mass spectra. Anal. Chem. 73, 4676–4681.

Janhom, T., Wattanachira, S., Pavasant, P., 2009. Characterization of brewery wastewater with spectrofluorometry analysis. J. Environ. Manag. 90 (2), 1184–1190.

Jani, J., et al., 2020. Wet season nitrogen export from a residential stormwater pond. PLoS One 15 (4), e0230908.

Kaiser, N.K., et al., 2011a. Electrically compensated Fourier transform ion cyclotron resonance cell for complex mixture mass analysis. Anal. Chem. 83 (17), 6907–6910.

Kaiser, N.K., et al., 2011b. A Novel 9.4 Tesla FT ICR mass spectrometer with improved sensitivity, mass resolution, and mass range. J. Am. Soc. Mass Spectrom. 22 (8), 1343–1351.

Kaiser, N.K., et al., 2013. Tailored ion radius distribution for increased dynamic range in FT-ICR mass analysis of complex mixtures. Anal. Chem. 85 (1), 265–272.

Kaiser, N.K., Savory, J.J., Hendrickson, C.L., 2014a. Controlled ion ejection from an external trap for extended m/z range in FT-ICR mass spectrometry. J. Am. Soc. Mass Spectrom. 25 (6), 943–949.

Kaiser, N.K., Savory, J.J., Hendrickson, C.L., 2014b. Controlled ion ejection from an external trap for extended m/z range in FT-ICR mass spectrometry. J. Am. Soc. Mass Spectrom. 25, 943–949.

Kaushal, S.S., Belt, K.T., 2012. The urban watershed continuum: evolving spatial and temporal dimensions. Urban Ecosyst. 15 (2), 409–435.

Kendrick, E., 1963. A mass scale based on $CH_2 = 14.0000$ for high resolution mass spectrometry of organic compounds. Anal. Chem. 35 (13), 2146–2154.

Killberg-Thoreson, L., et al., 2014a. Nitrogen uptake kinetics in field populations and cultured strains of *Karenia brevis*. Harmful Algae 38, 73–85.

Killberg-Thoreson, L., et al., 2014b. Nutrients released from decaying fish support microbial growth in the eastern Gulf of Mexico. Harmful Algae 38, 40–49.

Kim, S., Kramer, R., Hatcher, P., 2003. Graphical method for analysis of ultrahigh-resolution broadband mass spectra of natural organic matter, the van Krevelen diagram. Anal. Chem. 75 (20), 5336–5344.

Koch, B.P., Dittmar, T., 2006. From mass to structure: an aromaticity index for high-resolution mass data of natural organic matter. Rapid Commun. Mass Spectrom. 20 (5), 926–932.

Kovács, K., et al., 2010. Comparison of humic substances isolated from thermal water and surface water by electrospray ionization Fourier transform ion cyclotron resonance mass spectrometry. Eur. J. Mass Spectrom. 16 (5), 625–630.

Kujawinski, E.B., 2002. Electrospray ionization Fourier transform ion cyclotron resonance mass spectrometry (ESI FT-ICR MS): characterization of complex environmental mixtures. Environ. Forensic 3 (3–4), 207–216.

Langeland, K.A., 2014. Aquatic Pest Control Training Manual (Aquatic Category Exam) SM 3. University of Florida.

Larkin, S.L., Adams, C.M., 2013. Economic consequences of harmful algal blooms: literature summary. In: Economics of Harmful Algal Blooms: Literature Review. Final Report for Gulf of Mexico Alliance Project, p. 100304.

Lewitus, A.J., et al., 2008. Lagoonal stormwater detention ponds as promoters of harmful algal blooms and eutrophication along the South Carolina coast. Harmful Algae 8 (1), 60–65.

Liu, C., et al., 2023. Microbial transformation of dissolved organic sulfur during the oxic process in 47 full-scale municipal wastewater treatment plants. Environ. Sci. Technol. 57 (5), 2118–2128.

Lusk, M., Toor, G., 2016a. Biodegradability and molecular composition of dissolved organic nitrogen in urban stormwater runoff and outflow water from a stormwater retention pond. Environ. Sci. Technol. 50 (7), 3391–3398.

Lusk, M., Toor, G., 2016b. Dissolved organic nitrogen in urban streams: biodegradability and molecular composition studies. Water Res. 96, 225–235.

Lusk, M.G., Toor, G.S., Inglett, P.W., 2020. Organic nitrogen in residential stormwater runoff: implications for stormwater management in urban watersheds. Sci. Total Environ. 707, 135962.

Lusk, M.G., Garzon, P.S., Muni-Morgan, A., 2023. Nitrogen forms and dissolved organic matter optical properties in bulk rainfall, canopy throughfall, and stormwater in a subtropical urban catchment. Sci. Total Environ. 896, 165243.

McLafferty, F.W., Turecek, F., 1993. Interpretation of Mass Spectra, 4th ed. University Science Books, Mill Valley, CA.

Nebbioso, A., et al., 2014. Molecular characterization of an end-residue of humeomics applied to a soil humic acid. RSC Adv. 4 (45), 23658–23665.

Osburn, C.L., et al., 2016. Predicting sources of dissolved organic nitrogen to an estuary from an agro-urban coastal watershed. Environ. Sci. Technol. 50 (16), 8473–8484.

Palenik, B., Morel, F.M., 1990. Amino acid utilization by marine phytoplankton: a novel mechanism. Limnol. Oceanogr. 35 (2), 260–269.

Pehlivanoglu-Mantas, E., Sedlak, D.L., 2008. Measurement of dissolved organic nitrogen forms in wastewater effluents: concentrations, size distribution and NDMA formation potential. Water Res. 42 (14), 3890–3898.

Rook, J.J., 1976. Haloforms in drinking water. J. Am. Water Work. Assoc. 68 (3), 168–172.

Rosenzweig, B.R., et al., 2011. Monitoring nitrogen loading and retention in an urban strormwater detention pond. J. Environ. Qual. 40, 598–609.

Savory, J.J., et al., 2011. Parts-Per-Billion Fourier transform ion cyclotron resonance mass measurement accuracy with a "Walking" calibration equation. Anal. Chem. 83 (5), 1732–1736.

Seitzinger, S.P., Sanders, R., Styles, R., 2002. Bioavailability of DON from natural and anthropogenic sources to estuarine plankton. Limnol. Oceanogr. 47 (2), 353–366.

Sinclair, J.S., et al., 2020. Stormwater ponds: an overlooked but plentiful urban designer ecosystem provides invasive plant habitat in a subtropical region (Florida, USA). Sci. Total Environ. 711, 135133.

Sipler, R.E., 2009. The Role of Dissolved Organic Matter in Structuring Microbial Community Composition. The State University of New Jersey, School of Graduate Studies, Rutgers.

Sipler, R.E., et al., 2013. *Trichodesmium*-derived dissolved organic matter is a source of nitrogen capable of supporting the growth of toxic red tide *Karenia brevis*. Mar. Ecol. Prog. Ser. 483, 31–45.

Sleighter, R.L., Hatcher, P.G., 2011. Fourier transform mass spectrometry for the molecular level characterization of natural organic matter: instrument capabilities, applications, and limitations. In: Fourier Transforms-Approach to Scientific Principles, pp. 295–320.

Sleighter, R.L., et al., 2012. Establishing a measure of reproducibility of ultrahigh-resolution mass spectra for complex mixtures of natural organic matter. Anal. Chem. 84 (21), 9184–9191.

Soule, M.C.K., et al., 2010. Impact of instrument and experiment parameters on reproducibility of ultrahigh resolution ESI FT-ICR mass spectra of natural organic matter. Org. Geochem. 41 (8), 725–733.

Sunda, W., et al., 2002. An antioxidant function for DMSP and DMS in marine algae. Nature 418 (6895), 317–320.

Van Dolah, F.M., et al., 2009. The Florida red tide dinoflagellate *Karenia brevis*: new insights into cellular and molecular processes underlying bloom dynamics. Harmful Algae 8 (4), 562–572.

Vargo, G., et al., 1992. Review and Synthesis of Historical Tampa Bay Water Quality Data. Final Technical Report.

Vargo, G.A., et al., 2004. Four *Karenia brevis* blooms: a comparative analysis. In: Harmful Algae 2002 Proceedings of the Xth International Conference on Harmful Algae, Florida Fish and Wildlife Conservation Commission, Florida Institute of Oceanography, and the Intergovernmental Oceanographic Commission of UNESCO, St. Petersburg (FL).

Vargo, G.A., et al., 2008. Nutrient availability in support of *Karenia brevis* blooms on the central West Florida Shelf: what keeps *Karenia* blooming? Cont. Shelf Res. 28 (1), 73–98.

Wang, X., et al., 2018. Molecular characterization of effluent organic matter in secondary effluent and reclaimed water: comparison to natural organic matter in source water. J. Environ. Sci. 63, 140–146.

Wang, X., et al., 2023. Formation of microorganism-derived dissolved organic nitrogen in intermittent aeration constructed wetland and its stimulating effect on phytoplankton production: implications for nitrogen mitigation. Water Res. 230, 119563.

Williams, C.J., Frost, P.C., Xenopoulos, M.A., 2013. Beyond best management practices: pelagic biogeochemical dynamics in urban stormwater ponds. Ecol. Appl. 23 (6), 1384–1395.

Yan, C., et al., 2022. Algal/bacterial uptake kinetics of dissolved organic nitrogen in municipal wastewater treatment facilities effluents. J. Environ. Manag. 309, 114719.

Yang, R., et al., 2021. Influences of the hydrophilic components of two anthropogenic dissolved organic nitrogen groups on phytoplankton growth in Jiaozhou Bay, China. Mar. Pollut. Bull. 169, 112551.

Yao, X., et al., 2020. Emerging role of dissolved organic nitrogen in supporting algal bloom persistence in Lake Taihu, China: emphasis on internal transformations. Sci. Total Environ. 736, 139497.

Young, H.W., York, D.W., 1996. Reclaimed water reuse in Florida and the South Gulf Coast. Florida Water Resour. J 32–36.

Zhang, B., et al., 2021. Unravelling molecular transformation of dissolved effluent organic matter in UV/H_2O_2, UV/persulfate, and UV/chlorine processes based on FT-ICR-MS analysis. Water Res. 199, 117158.